

A Mn₁₇ Octahedron with a Giant Ground-State Spin: Occurrence in Discrete Form and as Multidimensional Coordination Polymers

Eleni E. Moushi,[†] Theocharis C. Stamatatos,[‡] Wolfgang Wernsdorfer,[§] Vassilios Nastopoulos,^{||} George Christou,^{**‡} and Anastasios J. Tasiopoulos^{**†}

[†]Department of Chemistry, University of Cyprus, 1678 Nicosia, Cyprus, [‡]Department of Chemistry, University of Florida, Gainesville, Florida 32611-7200, [§]Institut Néel, CNRS, BP-166, Grenoble Cedex 9, France, and ^{||}Department of Chemistry, University of Patras, 26500 Patras, Greece

Received September 19, 2008

A [Mn^{III}Mn^{II}(μ₄-O)₈(μ₃-L)₄]²⁵⁺ (L = N₃⁻ or OCN⁻) octahedral unit is reported, occurring within 1D (**1**)_∞ and 2D (**2**)_∞ coordination polymers, as well as the corresponding 0D discrete cluster **3**. It possesses a giant ground-state spin value, determined in the case of **3** to be S = 37, the second largest to be reported to date. In addition, compound **3** displays single-molecule magnet (SMM) behavior, and is thus the largest-spin SMM.

Paramagnetic transition-metal clusters continue to attract great attention, mainly because of their often unusual and sometimes novel magnetic properties.^{1,2} Such molecules may exhibit high and sometimes abnormally high ground-state spin values, currently up to S = 83/2.¹ Several such clusters are now known, including the Mn₁₉ family with S = 83/2¹ and 73/2³ and the Mn₂₅ family with S = 51/2⁴ and 61/2,⁵ but it is still very difficult to predict what type of structure will give a large S. There are, however, some strategies that can assist the synthesis of new high-spin molecules, and these include the use of bridging ligands that result in ferromagnetic interactions. The best ligand for this is the N₃⁻ group when it bridges metal ions in the end-on (1,1) fashion.⁶ We have thus included this group in our systematic investigation of the use of 1,3-propanediol (pdH₂) and its derivatives in manganese carboxylate chemistry.⁷ We herein report three new compounds that all contain the same new Mn₁₇ cluster but that differ in their dimensionality: the 1D [Mn₁₇O₈-

(N₃)₅(O₂CMe)₄(pd)₁₀(py)₆]_∞ (**1**)_∞ and 2D [Mn₁₇O₈(OCN)₇(O₂CMe)₂(pd)₁₀(py)₄]_∞ (**2**)_∞ coordination polymers and the corresponding 0D discrete cluster [Mn₁₇O₈(N₃)₄(O₂CMe)₂(pd)₁₀(py)₁₀(MeCN)₂(H₂O)₂](ClO₄)₃ (**3**). All three compounds contain the high-symmetry [Mn^{III}Mn^{II}(μ₄-O)₈(μ₃-L)₄]²⁵⁺ [L = N₃⁻ (**1** and **3**), OCN⁻ (**2**)] octahedral unit, which possesses a giant ground-state spin that for discrete **3** was determined to be S = 37, the second largest to date. In addition, compound **3** displays single-molecule magnet (SMM) behavior and is thus the largest-spin SMM known to date.

Compound (**1**)_∞ was the first one isolated: it was obtained in 30% yield from the reaction of [Mn(O₂CMe)₂]·4H₂O, pdH₂, and NaN₃ (1:5:1) in MeCN/py (py = pyridine). Magnetic susceptibility and X-ray crystallographic studies (vide infra) clearly suggested that the Mn₁₇ repeating unit of **1** possesses a large ground-state spin S, but its exact value was impossible to determine because of the covalent linkage of neighboring Mn₁₇ units, which introduced intermolecular magnetic interactions. The isolation of this Mn₁₇ unit in a discrete form was thus targeted with high priority. Because the Mn₁₇ units in (**1**)_∞ were connected by 1,3-bridging N₃⁻ groups, we explored the analogous reactions with OCN⁻ with the hope that OCN⁻ would still bridge intramolecularly but preclude the μ-1,3 (end-to-end) bridging of neighboring Mn₁₇ units and thus avoid the formation of a polymeric species. However, the use of OCN⁻ gave instead the 2D coordination polymer (**2**)_∞ in 32% yield, with properties very similar to those of (**1**)_∞. The second and successful strategy was to include an excess of a poorly coordinating counteranion such as ClO₄⁻ in order to stabilize a positively charged species that might contain neutral terminal ligands instead of the μ-1,3 N₃⁻ groups. Thus, the reaction of [Mn(O₂CMe)₂]·4H₂O with pdH₂ in the presence of NaN₃ and Mn(ClO₄)₂·6H₂O in a 1:5:1:1 molar ratio in MeCN/py and subsequent diffusion of Et₂O into the yellow solution led to the isolation of **3** in 30% yield after a few days.

The structures of (**1**)_∞ [Figure S1 in the Supporting Information (SI)],⁸ (**2**)_∞ (Figure S2 in the SI),⁸ and **3**⁸ (Figure 1,

*To whom correspondence should be addressed. E-mail: atasio@ucy.ac.cy (A.J.T.), christou@chem.ufl.edu (G.C.).

(1) Ako, A. M.; Hewitt, I. J.; Mereacre, V.; Clérac, R.; Wernsdorfer, W.; Anson, C. E.; Powell, A. K. *Angew. Chem., Int. Ed.* **2006**, *45*, 4926.

(2) Aromi, G.; Brechin, E. K. *Struct. Bonding (Berlin)* **2006**, *1*, 1.

(3) Ge, C.-H.; Ni, Z.-H.; Liu, C.-M.; Cui, A.-L.; Zhang, D.-Q.; Kou, H.-Z. *Inorg. Chem. Commun.* **2008**, *11*, 675.

(4) Murugesu, M.; Takahashi, S.; Wilson, A.; Abboud, K. A.; Wernsdorfer, W.; Hill, S.; Christou, G. *Inorg. Chem.* **2008**, *47*, 9459.

(5) Stamatatos, T. C.; Abboud, K. A.; Wernsdorfer, W.; Christou, G. *Angew. Chem., Int. Ed.* **2007**, *46*, 884.

(6) Escuer, A.; Aromi, G. *Eur. J. Inorg. Chem.* **2006**, 4721.

(7) (a) Moushi, E. E.; Stamatatos, T. C.; Wernsdorfer, W.; Nastopoulos, V.; Christou, G.; Tasiopoulos, A. J. *Angew. Chem., Int. Ed.* **2006**, *45*, 7722.

(b) Moushi, E. E.; Lampropoulos, C.; Wernsdorfer, W.; Nastopoulos, V.; Christou, G.; Tasiopoulos, A. J. *Inorg. Chem.* **2007**, *46*, 3795.

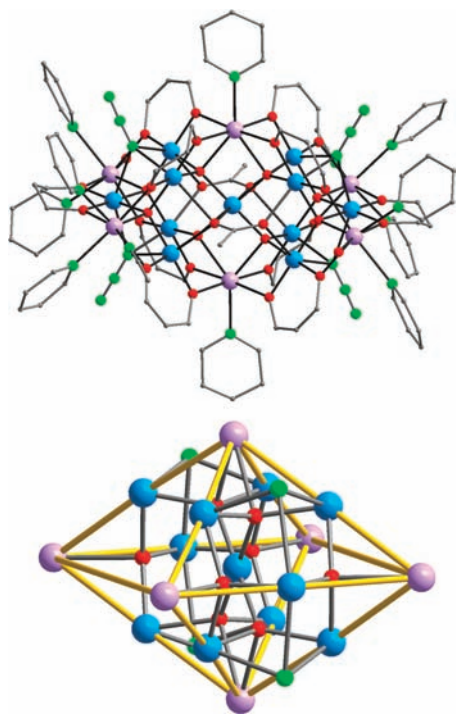


Figure 1. Structure of **3** (top) and its core (bottom). In the lower figure, the yellow line connecting the Mn ions is to emphasize the octahedral topology. Color scheme: Mn^{III}, blue; Mn^{II}, purple; O, red; N, green; C, gray. H atoms have been omitted for clarity.

top) all contain a $[\text{Mn}_{17}(\mu_4\text{-O})_8(\mu_3\text{-L})_4(\text{pd})_{10}(\text{O}_2\text{CMe})_2]^{3+}$ unit with a flattened octahedral topology. Bond valence sum (BVS) calculations,⁹ charge considerations, and inspection of metric parameters reveal a mixed-valence Mn^{III}Mn^{II} situation. The 17 Mn ions of the core (Figure 1, bottom) are disposed in alternating Mn/Mn₄/Mn₇/Mn₄/Mn layers: the Mn₄ layers are nearly planar rectangles; the central Mn₇ layer is also a rectangle, this time comprising six Mn ions with a seventh at its center, and the remaining two Mn ions occupy the top and bottom capping positions. The Mn₁₇ core is held together by eight $\mu_4\text{-O}^{2-}$ and four $\mu_3\text{-1,1,1-N}_3^-$ (or OCN^-) bridging ligands. The structures also contain 10 pd^{2-} and two carboxylate bridging ligands. For compound **1**, the peripheral ligation is completed by six terminal pyridine, two chelating acetate, and one $\mu\text{-1,3-N}_3^-$ ligands. The latter bridges Mn7 of one Mn₁₇ unit to its symmetry-related Mn ion of a neighboring Mn₁₇ unit, resulting in the formation of a 1D coordination polymer (Figure 2, top). The shortest Mn \cdots Mn separation between different Mn₁₇ units is ~ 6.24 Å. For compound **2**, the peripheral ligation is completed by four terminal pyridine and three $\mu\text{-1,3-OCN}^-$ ligands. The three OCN^- groups bridge two Mn ions of the Mn₁₇ unit (Mn7 and Mn9) with Mn ions of two neighboring Mn₁₇ units, resulting in a 2D coordination polymer (Figure 2, bottom). The shortest Mn \cdots Mn separation between different Mn₁₇ units is ~ 6.36 Å. For compound **3**, the peripheral ligation is completed by 10 pyridine, 2 water and 2 MeCN ligands, all terminal. A close examination of the packing of **3** reveals the existence of intermole-

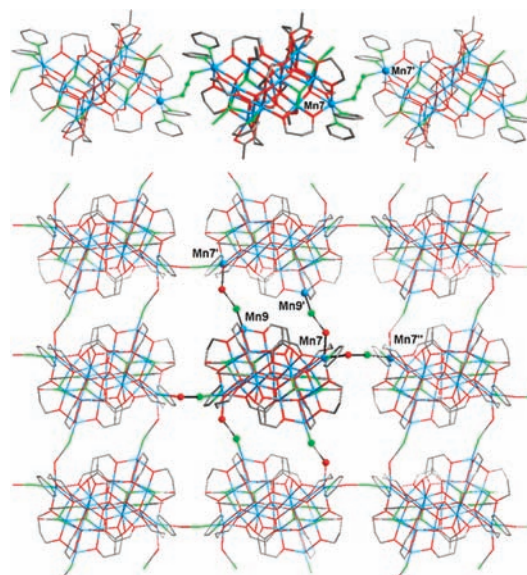


Figure 2. Wireframe representations of sections of **(1)**_∞ (top) and **(2)**_∞ (bottom) emphasizing the connection of Mn₁₇ units into 1D and 2D polymeric networks, respectively. The color scheme is as in Figure 1.

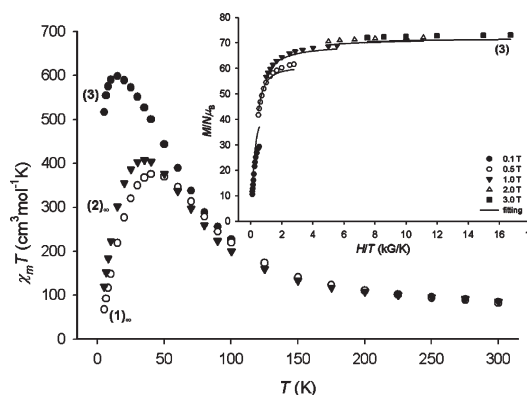


Figure 3. $\chi_m T$ vs T plots for **(1)**_∞, **(2)**_∞, and **3**. Inset: Plot of reduced magnetization, $M/N\mu_B$ vs H/T for **3**. The solid lines are the fit; see the text for the fit parameters.

cular hydrogen-bonding interactions involving terminally bound and lattice H₂O molecules and ClO_4^- counterions ($\text{O}\cdots\text{O}$ separations = 2.7–2.9 Å); i.e., there are no hydrogen bonds directly between neighboring Mn₁₇ cations, and as a result, the shortest Mn \cdots Mn separation between different Mn₁₇ units is ~ 8.47 Å, significantly longer than those for **(1)**_∞ and **(2)**_∞.

Solid-state direct current (dc) magnetic susceptibility measurements were performed on vacuum-dried microcrystalline samples of **(1)**_∞,^{10a} **(2)**_∞,^{10b} and **3**^{10c} in a 0.1 T field in the 5–300 K range. The obtained data are shown as $\chi_m T$ vs T plots in Figure 3, and they indicate the existence of predominantly ferromagnetic interactions and a resulting giant ground-state spin for the Mn₁₇ units. For **(1)**_∞ and **(2)**_∞, $\chi_m T$ increases from 82.5 and 85.9 $\text{cm}^3 \text{mol}^{-1} \text{K}$ at 300 K to maxima of 375.4 and 407.5 $\text{cm}^3 \text{mol}^{-1} \text{K}$ at 40 and 35 K, respectively, before decreasing rapidly to 67.9 and 119.0 $\text{cm}^3 \text{mol}^{-1} \text{K}$ at 5 K. The low-temperature decrease is very probably due to intermolecular antiferromagnetic exchange interactions mediated by the end-to-end N_3^- and OCN^- ligands, resulting in diamagnetic ground spin states for the two polymeric species. For **3**,

(8) The Crystal data for $(1 \cdot 2\text{H}_2\text{O} \cdot 2\text{MeCN})_\infty$, $(2 \cdot 1\text{H}_2\text{O})_\infty$ and $3 \cdot 1.2\text{H}_2\text{O}$ are provided in the Supporting Information.

(9) (a) BVS calculations for the Mn^{9b} ions of compounds **(1)**_∞, **(2)**_∞, and **3** gave oxidation state values of 2.83–3.16 (Mn^{III}) and 1.81–2.07 (Mn^{II}). (b) Liu, W.; Thorp, H. H. *Inorg. Chem.* **1993** *32*, 4102.

$\chi_m T$ increases from $83.9 \text{ cm}^3 \text{ mol}^{-1} \text{ K}$ at 300 K to a maximum of $597.9 \text{ cm}^3 \text{ mol}^{-1} \text{ K}$ at 15 K before decreasing to $516.6 \text{ cm}^3 \text{ mol}^{-1} \text{ K}$ at 5 K. The maximum is consistent with an $S = 37$ ground state, the maximum possible for a $\text{Mn}_{11}^{\text{III}}\text{Mn}_6^{\text{II}}$ system, assuming a g value of slightly less than 2. The low-temperature decrease is due to Zeeman effects, zero-field splitting, and/or weak intermolecular interactions. dc magnetization data were collected in the temperature and magnetic field ranges of 1.8–10 K and 0.1–7 T, respectively. The data were fit by assuming that only the ground state is populated and by including axial zero-field-splitting ($D\hat{S}_z^2$) and Zeeman interactions. For the two polymeric species ($\mathbf{1}$) $_{\infty}$ and ($\mathbf{2}$) $_{\infty}$, the intermolecular interactions of significant strength between neighboring Mn_{17} molecules precluded a fit of the data to isolated units,^{7b} but for $\mathbf{3}$, a good fit was obtained with $S = 37$, $g = 1.95$, and $D = -0.009 \text{ cm}^{-1}$ (Figure 3, inset).

The conclusions from the dc studies were also confirmed by alternating current (ac) susceptibility experiments. The in-phase $\chi_m' T$ (Figure S3 in the SI) for the two polymeric species decreases almost linearly with decreasing temperature and is clearly heading to $\chi_m' T$ values close to zero at 0 K consistent with antiferromagnetic intermolecular interactions and a diamagnetic ground spin state. Extrapolation of the $\chi_m' T$ signal of $\mathbf{3}$ (Figure S3 in the SI) to 0 K from above 8 K to avoid the effects of intermolecular interactions gave $\chi_m' T \sim 620 \text{ cm}^3 \text{ mol}^{-1} \text{ K}$, consistent with $S \sim 37$ and g slightly less than 2.0 ($\chi_m' T$ for an $S = 37$ state with $g = 1.88$ is $621.2 \text{ cm}^3 \text{ mol}^{-1} \text{ K}$), as expected for a $\text{Mn}^{\text{II}}/\text{Mn}^{\text{III}}$ complex. The lowest temperature decrease is likely due to weak intermolecular interactions between neighboring Mn_{17} units and is also typical of other high-spin molecules.^{4,5} For all three complexes, there is no ac out-of-phase (χ_m'') signal down to 1.8 K (Figures S4–S6 in the SI).

The $S = 37$ ground state and negative D value suggested that $\mathbf{3}$ might be an SMM. Single-crystal magnetic studies on $\mathbf{3} \cdot 1.2\text{H}_2\text{O}$ were therefore performed using a micro-SQUID instrument,¹¹ and magnetization (M) vs dc field sweeps are shown in Figure 4. Hysteresis loops are evident below ~ 0.7 K, with their coercivities increasing with decreasing temperature, as expected for an SMM. An Arrhenius plot constructed from dc magnetization decay data gave $U_{\text{eff}} = 9.0 \text{ cm}^{-1} = 13 \text{ K}$ and $\tau_0 = 1.0 \times 10^{-13} \text{ s}$, where τ_0 is the preexponential factor (Figures S7 and S8 in the SI). The small value of τ_0 , smaller than is typical for purely SMM behavior,² is likely due to weak intermolecular interactions and low-lying excited states; large clusters often give smaller τ_0 values.^{4,5} Note that adjacent Mn_{17} clusters in $\mathbf{3}$ are hydrogen-bonded in one direction, but not directly, only via the lattice H_2O molecules. Thus, intermolecular exchange interactions will be very weak,

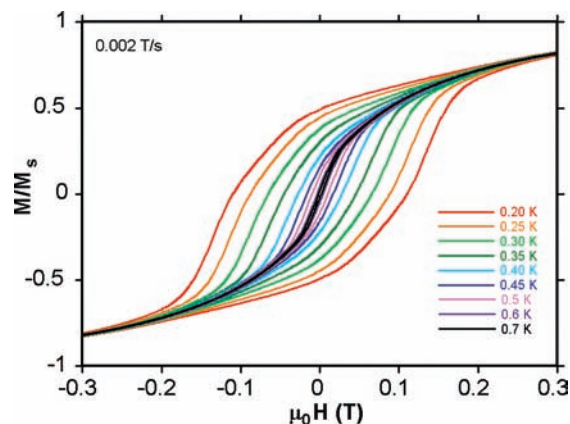


Figure 4. Magnetization (M) versus field hysteresis loops for single crystals of $\mathbf{3} \cdot 1.2\text{H}_2\text{O}$ at the indicated temperatures. The magnetization is normalized to its saturation value (M_s).

and they will represent merely perturbations of single-molecule properties. In addition, they will be antiferromagnetic and thus could not make $\mathbf{3}$ be a single-chain magnet rather than an SMM.

In summary, the use of $\text{N}_3^-/\text{OCN}^-$ ligands in Mn-pdH_2 chemistry under various conditions has yielded essentially the same Mn_{17} unit within 0D, 1D, and 2D compounds. The discrete form $\mathbf{3}$ was targeted once the polymeric form was identified, and it was obtained by a procedure containing some elements of synthetic control that could also prove useful for the isolation in discrete form of the repeating cluster of other coordination polymers. Compound $\mathbf{3}$ possesses a giant ground-state spin of $S = 37$ and is the largest-spin SMM to date. $S = 37$ is also the second-highest ground state yet identified,¹ and it is the maximum for a $[\text{Mn}_{11}^{\text{III}}\text{Mn}_6^{\text{II}}]$ species, thus indicating that most, if not all, of the interactions are ferromagnetic. This is consistent with the $\mu_3-1,1,1-\text{N}_3^-$ ligands, which are known to mediate ferromagnetic interactions.⁶ Finally, the labile terminal ligands on the Mn_{17} units offer a variety of additional possibilities for crystal engineering, i.e., introducing interunit linkages of various types for the construction of multidimensional coordination polymers with interesting magnetic and/or structural properties. Compounds ($\mathbf{1}$) $_{\infty}$ and ($\mathbf{2}$) $_{\infty}$ provide a proof-of-feasibility of this strategy that encourages us to believe an expanded family of related polymeric species containing this high-spin Mn_{17} unit should be possible.

Acknowledgment. This work was supported by the Cyprus Research Promotion Foundation and the National Science Foundation.

Supporting Information Available: Crystallographic details (CIF), structural representations, and magnetism plots. This material is available free of charge via the Internet at <http://pubs.acs.org>.

(10) (a) It analyzes as $\mathbf{1} \cdot 2\text{H}_2\text{O}$. (b) It analyzes as $\mathbf{2} \cdot 6\text{H}_2\text{O}$. (c) It analyzes as $\mathbf{3} \cdot 4\text{H}_2\text{O}$.

(11) Wernsdorfer, W. *Adv. Chem. Phys.* **2001**, *118*, 99.